Available online at www.sciencedirect.com
ScienceDirect
Journal of Power Sources 174 (2007) 400–407
JOURNAL OF POWER SOURCES
www.elsevier.com/locate/jpowsour

# On the electrochemical and thermal behavior of lithium bis(oxalato)borate (LiBOB) solutions

L. Larush-Asraf, M. Biton, H. Teller, E. Zinigrad *, D. Aurbach

*Department of Chemistry, Bar-Ilan University, Ramat-Gan 52900, Israel*

Available online 29 June 2007

**Abstract**

In recent years, lithium bis(oxalato)borate, $LiB(C_2O_4)_2$ (LiBOB) has been proposed as an alternative salt to the commonly used electrolyte, $LiPF_6$. There is evidence of the enhanced stability of Li-ion battery electrodes in solutions of this salt, due to a unique surface chemistry developed in LiBOB solutions. The present study is aimed at further exploring the electrochemical and thermal properties of LiBOB solutions in mixtures of alkyl carbonates with non-active metal, graphite and lithium electrodes. FTIR spectroscopy, XPS, EQCM, *in situ* AFM imaging, and DSC were used in conjunction with standard electrochemical techniques. The study also included a comparison between LiBOB and $LiPF_6$ solutions. The development of a favorable surface chemistry in LiBOB solutions that provides better passivation to Li and Li-graphite electrodes was clearly evident.


*Keywords:* LiBOB; Graphite; EQCM; AFM; Thermal analysis

## 1. Introduction

$LiPF_6$ is the commonly used electrolyte in Li-ion batteries [1]. Its solutions in alkyl carbonate mixtures can reach a high specific conductivity (>10 mS $cm^{-1}$), and it does not significantly affect the electrochemical windows of its solutions, which are usually limited by solvent reactions (both anodic and cathodic). The performance of both lithiated graphite anodes and commonly used cathodes ($Li_xMO_2$, M = Mn, Co, Ni mixtures of transition metals, etc.) in $LiPF_6$ solutions is adequate for battery applications. There are, however, several drawbacks to the choice of this salt as a major Li battery electrolyte. The thermal stability of $LiPF_6$ solutions is very limited. All $LiPF_6$-alkyl carbonate solutions are red-ox couples in which the $PF_6$-anion is a strong oxidizer at elevated temperatures. Hence, $LiPF_6$-alkyl carbonate solutions may under thermal runaway upon heating, even without contact with electrodes [2]. The thermal stability of $LiPF_6$ solutions with lithiated graphite or delithiated transition metal oxides is even worse [3,4]. Hence, the use of $LiPF_6$ raises severe safety problems, especially for large battery applications. In addition, $LiPF_6$ undergoes thermal decomposition to form LiF and $PF_5$ [5]. The latter is highly sensitive to protic contaminants, and any contact between this gas and protic substances forms HF. In fact, all $LiPF_6$ solutions are unavoidably contaminated by HF [6]. The presence of HF in solutions has a detrimental impact on the surface chemistry of both anodes and cathodes. It badly affects the passivation of graphite electrodes [7] and promotes the dissolution of transition metal ions from cathode materials [8,9]. In fact, the presence of HF in $LiPF_6$ solutions may be considered as one of the main reasons for the limited performance of Li-ion batteries at elevated temperatures [10].

The above drawbacks of $LiPF_6$ solutions have promoted efforts to find replacements for this salt. A successful candidate was Merck's $LiPF_3(C_2F_5)_3$ (LiFAP) salt [11,12]. However, due to high production and purification costs, this excellent salt could not become a commercial product. In recent years, lithium bis(oxalato)borate, $LiB(C_2O_4)_2$ (LiBOB) was studied by several research groups and was found to be a highly interesting electrolyte for Li-ion batteries [13–20]. LiBOB solutions in alkyl carbonates were found to be much more thermally stable than $LiPF_6$ solutions [13,14]. The performance of lithiated graphite electrodes seems to be much better in LiBOB solutions than in all the other salts. Especially, striking is the fact that LiBOB is the only electrolyte with which lithium-graphite electrodes behave reversibly in single solvent propylene carbonate (PC) solutions [15,16]. In all other PC solutions with this solvent as a major

* Corresponding author.
*E-mail address:* zinigre@mail.biu.ac.il (E. Zinigrad).

0378-7753/$ – see front matter © 2007 Elsevier B.V. All rights reserved.
doi:10.1016/j.jpowsour.2007.06.171

component, composite graphite electrodes are destroyed during their first lithiation [21].

Despite the above-mentioned, intensive studies of LiBOB solutions and their many aspects, including their electrode surface chemistry [17,18], it is important to continue these rigorous studies on an extensive basis. This is because the use of LiBOB as a salt for Li-ion batteries, or even as a co-electrolyte or an additive, requires a thorough background of reliable and coherent data in order to facilitate appropriate and correct operational decisions. This paper reports on various studies related to LiBOB solutions, including aspects of surface chemistry, electrode performance and thermal stability. Electrodes for these studies included lithium, graphite (both synthetic flakes and mesocarbon microbeads—MCMB) and nickel. FTIR spectroscopy, XPS, electron microscopy, *in situ* AFM imaging, and EQCM were used, in conjunction with standard electrochemical techniques. DSC, ARC and TGA were used for the thermal studies of LiBOB salt and its solutions. In this paper, only the results from DSC studies are reported. In the studies reported herein, the behavior of LiBOB solutions was also compared to that of $LiPF_6$ and $LiClO_4$ solutions (in the same solvent mixtures).

## 2. Experimental

Highly purified LiBOB salt was obtained from Chemetall Inc. and was used as received. Solvents (Merck KGaA and Tomiyama) for solution preparation were of electrochemical purity grade. Solutions of 0.5 and 1 M LiBOB and 1 M $LiPF_6$ in PC, EC:DMC 1:1, and EC:PC 2:3 were prepared in a VAC glove box under a highly pure argon atmosphere. The surface films formed on polished, high purity nickel foil (Goodfellow) and polarized cathodically in LiBOB solutions were characterized by Fourier transform infrared (FTIR) spectroscopy (Magna 860 spectrometer from Nicolet Inc.) and placed in a glove box under $H_2O$- and $CO_2$-free atmosphere, and by XPS (Axis system from Kratos Inc.). EQCM measurements were performed using equipment from Elchema (EQCN 601 model, including a Farady cago). The electrodes used were 10 MHz (Elchema QC 10AU) AT cut quartz crystals of 14 mm diameter with 0.25 $cm^2$ active area, 10 microns thick, on which nickel was deposited. A differential scanning calorimeter (DSC), Model #822 from Mettler Toledo Inc., was used for the thermal analysis of LiBOB and $LiPF_6$ solutions. AFM measurements were carried out using the PicoSPM system from Molecular Imaging Inc. and were placed in the homemade glove box, with pyramidal silicon carbide tips [22]. In this study, we used the special electrochemical cells which we have discussed elsewhere [23]. The AFM images were obtained using the MI PicoScan Ver. 4.19 by $256^2$ points that were used for roughness calculations (built in, in the software). The cyclic voltammetry of MCMB electrodes were measured with a multichannel potentiostat-galvanostat, Model #1470, Solarton Inc. We used three-electrode coin-type cells (type 2032, standard product from NRC Inc., Canada), in which metallic lithium foil was used as counter and reference electrodes, as already described [24]. The electrodes were prepared by mixing the active material powder and a 10% PVdF binder and adding 1-methyl-2-pyrrolydone to obtain a homogeneous slurry which was then spread on a 12 mm diameter pre-rubbed copper disk. The electrodes' mass was usually 3–5 mg. The electrodes were dried under vacuum for 12 h.

## 3. Results and discussion

Figs. 1 and 2 show results from EQCM experiments with 0.5 M LiBOB, 1 M LiBOB, and 1 M $LiPF_6$ solutions in EC–DMC 1:1 (Fig. 1), and with 0.5 M LiBOB, 1 M LiBOB, and 1 M $LiClO_4$ solutions in EC–PC 2:3 (Fig. 2). Note that the mass accumulation as surface films and the currents measured, presented below, depends on the nature of the electrodes' passivation. This depends on both the reactivity of the solution species and the solubility of the reduction products.

It should be noticed that EC–PC solutions are very good probes for the study of the effects of morphology and the type of salt used, on the performance of graphite electrodes, better than any other solution. In EC–DMC–DEC, EMC solutions, most of graphite behaves well and the influence of the salt is small. In pure PC, most of graphite materials fail to insert reversibly lithium. Hence, in EC–PC, we have the positive effect of EC and negative effect of PC on the surface chemistry of graphite electrodes, at a delicate balance. This situation emphasizes strong effects of the salt used and the graphite's morphology on the electrodes' performance. Each chart shows the voltammetric response of a Ni-on-quartz crystal electrode, as well as the mass accumulation (and/or depletion) during cycling at 5 mV $s^{-1}$ in the potential range of 0–3 V versus $Li/Li^+$. The first three consecutive cycles are demonstrated. Hence, during the first cathodic polarization (1st cycle), the major surface film formation process takes place, as evident from the mass accumulation and the relatively high currents. There are significant differences in the behavior of the different solutions, which obviously reflect the different surface chemistry that is developed in each solution. In addition, it should be noted that the EC–PC mixture is more reactive towards reduction processes than EC–DMC (as PC is more reactive than DMC due to the ring's strain). All the voltammograms reflect the well-known behavior of noble [25,26] and Ni [27] electrodes in Li salt solutions of alkyl carbonate solvents. In general, pronounced broad cathodic peaks at potentials below 1.5 V ($Li/Li^+$) usually reflect the reduction of trace water and the onset of alkyl carbonate reduction. Then, the cathodic waves at potentials below 1.2 V belong to a gradual reduction of solution species, solvents, salt anions, trace water, and oxygen, as the potential is swept to more cathodic values [25,26]. The cathodic peaks around 0.6–0.5 V ($Li/Li^+$) and the corresponding anodic peaks between 1 and 1.2 V related to lithium UPD on nickel (followed by Li–Ni alloying) and the delithiation processes, respectively [27]. As seen from the charts in Figs. 1 and 2, mass accumulation on the electrodes during the first cathodic process starts at potentials below 2 V (can be attributed, in part, to trace oxygen reduction), accelerates at potentials below 1.4 V in all solutions, and may reach values of thousands of ng $cm^{-2}$ around 0 V. In the case of both 0.5 M LiBOB and 1 M $LiClO_4$ solutions in EC–PC mixtures, the accumulated mass remains steady during the consecutive anodic scan (first cycle). In the case of 0.5 M LiBOB EC–DMC solutions, mass also accumulates on

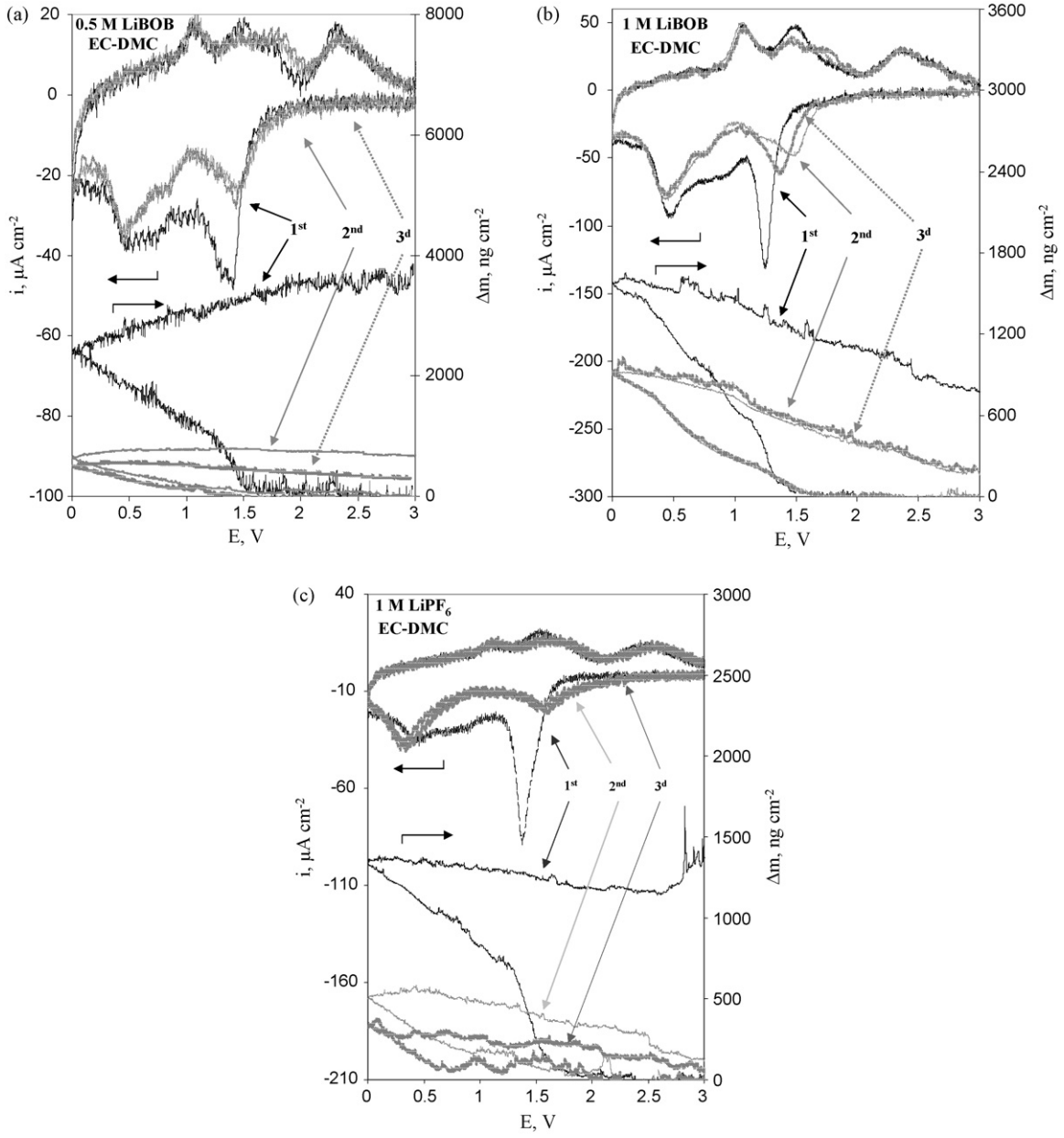


Fig. 1. Results of EQCM studies of: (a) 0.5 M LiBOB, (b) 1 M LiBOB, and (c) 1 M $LiPF_6$ solutions in EC–DMC 1:1. The first three consecutive CVs of nickel on quartz crystal electrodes and the mass response are presented, as indicated. 5 mV $s^{-1}$.

the electrode during the anodic scan. In the case of 1 M LiBOB solution mixtures (both in EC–PC and in EC–DMC), there is pronounced mass depletion during anodic scanning. Note that for the 1 M LiBOB solutions, the second and third consecutive CV cycles show nearly an identical, partially reversible mass response, namely, accumulation during cathodic scanning and a corresponding mass depletion during the anodic scanning.

The mass depletion means that there is an oxidation process of part of the surface species that forms soluble species. Hence, the reduction process that form surface films in that cases, is not fully irreversible as usual (for many Li salt/non-aqueous solutions). The response of the $LiPF_6$ solution also shows mass accumulation and a corresponding, very slight mass depletion during anodic scanning. However, it is significant that the mass response does not stabilize in the second cycle, as in the case of 1M LiBOB solutions.

The above results reflect the unique involvement of LiBOB in the surface chemistry of these systems. With 1 M LiBOB solutions in both EC–DMC and EC–PC mixtures, a pronounced mass depletion is recorded during the anodic scans. The system stabilizes in the second cycle, and a reversible slight mass accumulation–depletion is observed upon consecutive CV cycles (see, for example, Fig. 1b). It is clear that the surface reactivity of LiBOB is as high as that of EC–PC, which is considered to belong to the group of non-aqueous solvents most reactive towards electrochemical reduction (especially in the presence of Li ions) [28]. At first glance, the mass depletion observed in the EQCM experiments with 1 M LiBOB solutions may seem to

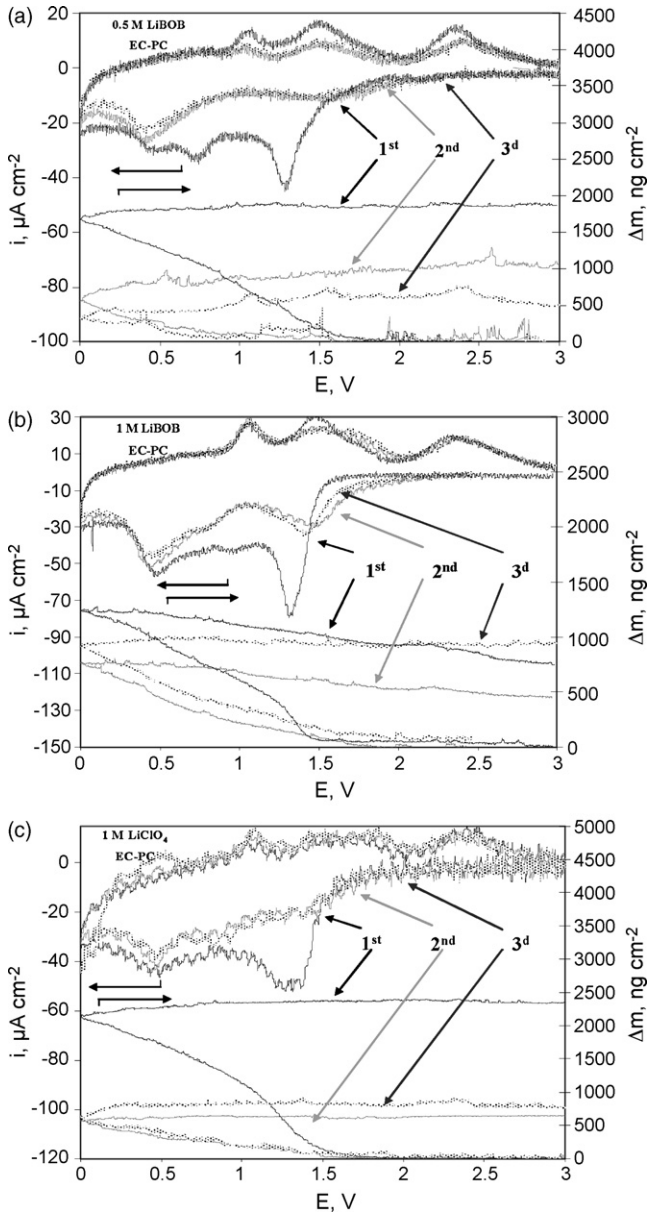


Fig. 2. Same as Fig. 1. EC–PC 2:3 solutions of: (a) 0.5, (b) 1 M LiBOB, and (c) 1 M $LiClO_4$, as indicated.

relate to the formation of surface species that are partially soluble in the solution. However, this is not the case for the Li alkyl carbonates formed by the reduction of the solvent molecules. Indeed, at a lower LiBOB concentration (0.5 M) and with $LiClO_4$ or $LiPF_6$ solutions, mass depletion is either not observed, or is very minor during anodic scans. However, it is also possible that the reversible mass accumulation–depletion seen in the second and third cycles in Fig. 1b (1 M LiBOB/EC–DMC solution) relates to reversible Li UPD, alloying with nickel, and the corresponding delithiating process, under conditions in which highly efficient passivation is achieved with surface films that are highly ion conducting. Indeed, measuring m.p.e. values (i.e., mass accumulated versus moles of electrons transferred, combining data from the quartz crystal frequency changes, and the electrode's electrochemical response [29] for these processes

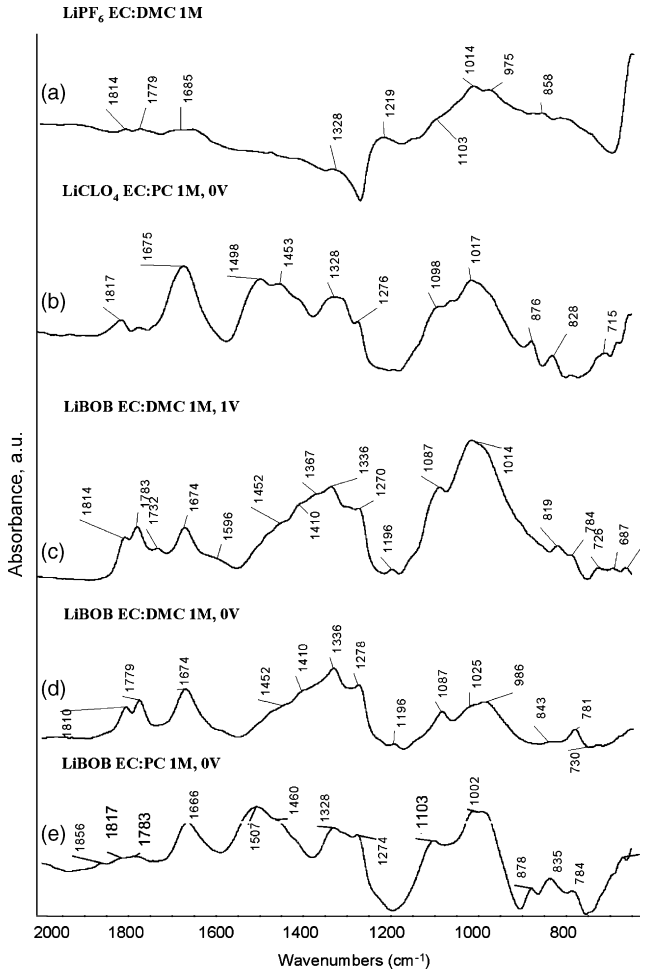


Fig. 3. FTIR spectrum measured from nickel mirror electrodes polarized from OCV (≈3 V) to low potential and in different solutions, as indicated. *Ex situ*, grazing angle (80°), external reflectance mode.

(Figs. 1b and 2b) shows numbers around 7–8 suitable for Li deposition/dissolution (e. g., through alloying and under potential deposition of Li with nickel at potentials higher then 0 V versus Li), while the m.p.e. values calculated for all the other solutions (Figs. 1a and c and 2a and c) are higher, around 13–24 for $LiPF_6$, 12–25 for $LiClO_4$ solutions, and 17–45 for 0.5 M LiBOB/EC–DMC solutions. XPS studies of these systems always show the presence of boron in the surface films formed on nickel electrodes polarized to low potentials in LiBOB solutions.

Fig. 3 shows FTIR spectra (*ex situ*, grazing angle reflectance mode) measured from nickel mirror electrodes polarized cathodically in LiBOB, $LiPF_6$ and $LiClO_4$ solutions. The most interesting range, 500–2000 $cm^{-1}$, is shown. Fig. 4 shows three reference FTIR spectra for comparison, that of LiBOB, Li oxalate ($Li_2C_2O_4$) and $(CH_2OCO_2Li)_2$, the major reduction product of EC on Li, Li-graphite and noble metal electrodes polarized to low potentials in EC–Li salt solutions (for more details see Ref. [28]). Based on previous studies, it is expected [30] that similar surface species are formed on these three types of electrodes in many polar aprotic Li salt solutions. The spectra in Fig. 3 are rich in peaks and reflect the formation of organic surface species, part of which can be identified. However, it should be noted that a rigorous analysis of these spectra is not

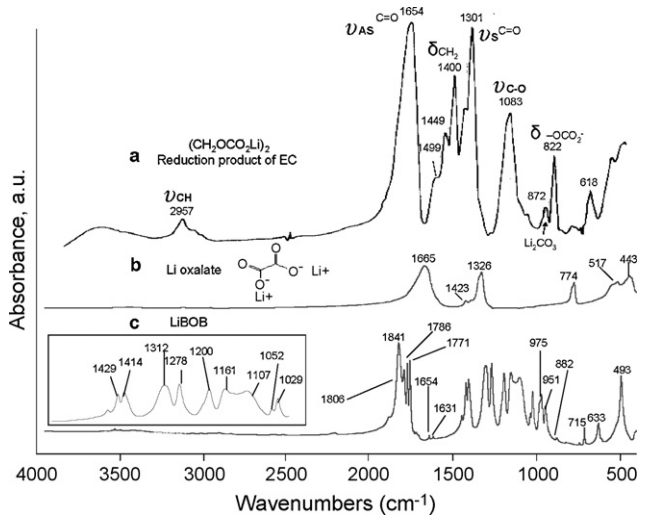


Fig. 4. Reference FTIR spectra of $(CH_2OCO_2Li)_2$, Li-oxalate and LiBOB in KBr pellets, transmittance mode, as indicated.

easy to achieve because several possible surface species that can be formed, including Li oxalate, $ROCO_2Li$ species, and LiBOB, have overlapping IR bands. In addition, Cl–O, P–O and B–O bands have pronounced peaks related to stretching modes around 1000–1100 $cm^{-1}$ [31,32] in the same region in which $ROCO_2Li$ and ROLi (other reduction products of alkyl carbonates, e.g., $CH_3OLi$ in the case of DMC) have pronounced IR peaks related to C–O stretching. Spectrum 3a, related to the $LiPF_6$ solution, does not show pronounced, well distinctive peaks because in this solution, when $ROCO_2Li$ surface species are formed, they react with trace HF to form surface LiF and $ROCO_2H$ in solution. Spectrum 3b, related to the $LiClO_4$ solution, belongs to $ROCO_2Li$, $Li_2CO_3$ and $LiClO_x$ surface species [25–30]. The latter compounds have pronounced Cl–O peaks around 1100–1000 $cm^{-1}$. $Li_2CO_3$ has typical too-broad peaks at 1500–1450 $cm^{-1}$ and another sharper and smaller peak around 870 $cm^{-1}$ [32]. The other peaks in this spectrum belong to $ROCO_2Li$ (compared with spectrum 4a). Spectra 3c–e related to the LiBOB solutions are all somewhat similar. One can easily recognize typical peaks of the expected $ROCO_2Li$ species formed by solvent reduction (compare with spectrum 4a with the peak assignments.

In all of the spectra related to LiBOB solutions, we can also recognize Li oxalate peaks (peaks around 780 and 1320–1330 $cm^{-1}$ can be distinguished, and the carboxylic peak around 1650 $cm^{-1}$ overlaps with that of $ROCO_2Li$). Pronounced peaks around 1000–1200 $cm^{-1}$ may relate to both $ROCO_2Li$ (see spectrum 4a) and B–O bonds (see spectrum 4c). Spectra 3c–e, which also contain peaks around 1750–1850 and 1270–1280 $cm^{-1}$, may also reflect the formation of several possible reduction products of LiBOB presented in Scheme 1 (based on a simple chemical logic). However, our spectral studies so far are not sufficiently conclusive to determine specifically all the major surface species. In any event, the EQCM, FTIR and XPS results show explicitly that LiBOB strongly influences the surface chemistry of these systems. Alkyl carbonate reduction may dominate the surface chemistry of LiBOB-alkyl carbonate solutions.

However, it is clear that LiBOB surface reactions also play an important role in determining the composition of the passivating films thus formed. Based on these and previous studies, it is expected that LiBOB reactions should have a pronounced impact on the surface chemistry of both lithium metal and lithiated carbon electrodes in LiBOB-alkyl carbonate solutions, despite the high reactivity of these solvents.

Our studies related to graphite electrodes with LiBOB solutions demonstrated that lithiated graphite electrodes function better in LiBOB solutions than in other Li salt solutions. Graphitic electrodes comprising both flakes (synthetic, natural) and MCMB undergo reversible intercalation in LiBOB-propylene carbonate solutions, while these electrodes fail in all other propylene carbonate solutions that contain any other Li salt. This unique advantage of LiBOB solutions is well documented in the literature [15,16]. The kinetics of graphite electrodes is faster in LiBOB solutions due to a better passivation

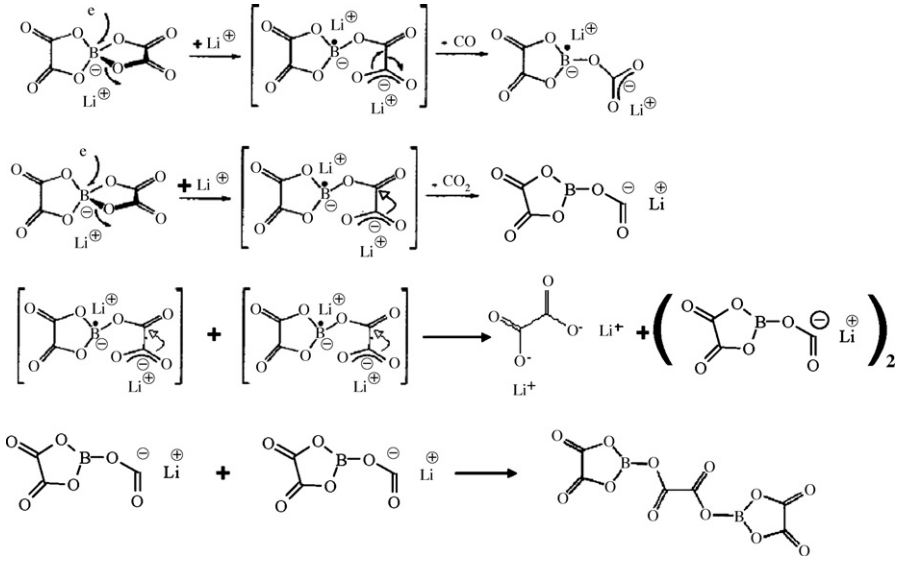

Scheme 1. Chemical reactions based on simple chemical logic.

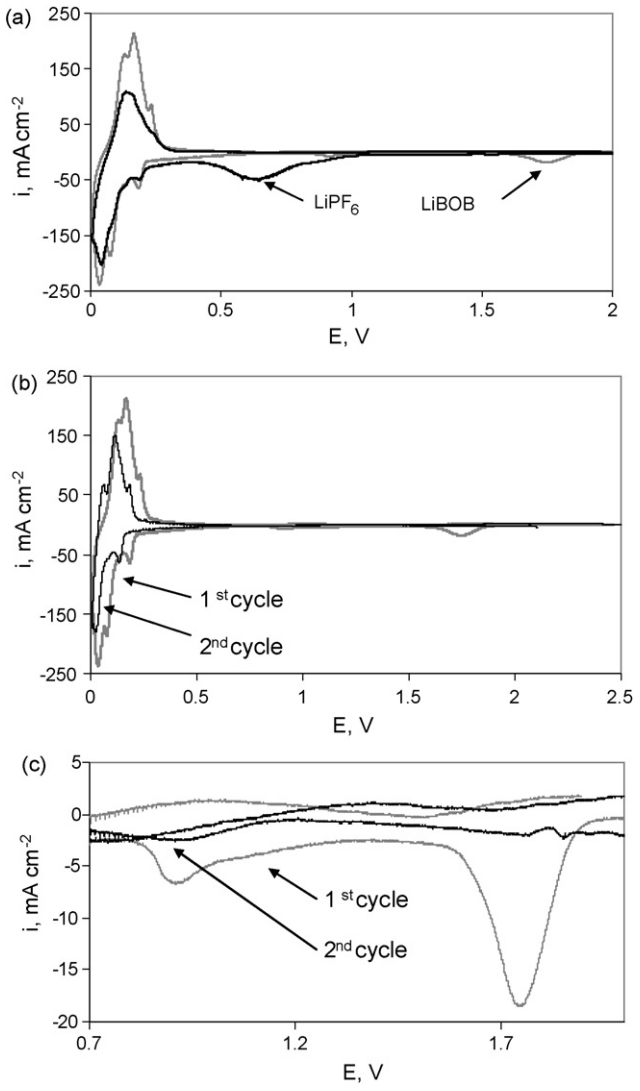


Fig. 5. CVs measured at 10 μV s$^{-1}$ with MCMB electrodes in 1 M LiBOB and 1 M $LiPF_6$ solutions in EC–PC 2:3. (a) Comparison of first CV of MCMB electrodes in LiBOB and $LiPF_6$ solutions. (b and c) Comparison of first and second consecutive CVs of MCMB electrodes in a 1M LiBOB EC–PC 2:3 solution.

in all commonly used standard solutions. This is well reflected by the voltammetric and chronopotentiometric response of graphite electrodes in these solutions. Sharper and better-resolved Li insertion peaks in CVs related to LiBOB solutions presented here, reflect better kinetics due to a lower impedance.

Fig. 5 shows cyclic voltammograms of composite graphite (MCMB) electrodes in EC–PC 2:3 solutions containing LiBOB or $LiPF_6$.

Fig. 5a compares first cycle CVs of graphite electrodes in 1M LiBOB and $LiPF_6$ solutions (EC–PC 2:3) and $LiPF_6$ solutions, and Figs. 5 b and c compare the first two consecutive CVs related to a graphite electrode in the 1 M LiBOB solution. The electrodes and experimental conditions were identical. However, it was clearly demonstrated that the CVs related to the LiBOB solution show sharper peaks (the peaks relate to the three major Li-graphite intercalation phase transition between diluted stage 1 → stage 4, stage 3 → stage 2, and stage 2 → stage 1). There are major irreversible processes related to the LiBOB and the $LiPF_6$ solutions around 1.7–1.8 and 0.5–1 V (very broad), respectively. In both solutions, these irreversible processes relate only to the first cathodic polarization of graphite electrodes when LiBOB solutions are used. However, with $LiPF_6$ solutions, passivation is reached after several consecutive charge–discharge cycles. The onset of alkyl carbonate solvent reduction in the presence of Li salts is usually below 1.5 V [25–27]. Hence, the fact that with LiBOB solutions a first reduction process appears around 1.7 V, means that a salt-induced process is the first cathodic reaction occurring upon the polarization of graphite electrodes from open circuit potential (OCP) towards intercalation potentials (<0.3 V versus Li/Li$^+$). Hence, LiBOB reduction processes probably dominate the surface chemistry of graphite electrodes in alkyl carbonate-based solutions [33].

This explains why even in PC/LiBOB solutions graphite electrodes behave so reversibly. In contrast, the initial surface chemistry of graphite electrodes in $LiPF_6$ solutions is dominated only by the solvents' reactions. The salt in this case affects mostly secondary reactions (HF reactions with surface species, see discussion above). Composite graphite electrodes comprising MCMB as the active mass were studied by *in situ* AFM imaging in EC–DMC and EC–PC solutions of LiBOB, $LiPF_6$ and $LiClO_4$ in an attempt to follow any pronounced morphological changes in the graphite particles, due to surface film formation (in the course of the first cathodic polarization) and during Li insertion and de-insertion processes. Graphite electrodes were first imaged dry, after which the solution was introduced and images of the electrodes at OCP were obtained. The electrodes were polarized to certain potentials and then were measured by AFM (*in situ*). The electrodes were also imaged during experiments by the CCD, which is a part of this instrument, and clearly showed phenomena such as gas evolution during the cathodic polarization of graphite electrodes. An obvious and clear result is that when graphite electrodes are polarized in LiBOB solutions, the gas evolution that usually accompanies the surface film formation in alkyl carbonates solutions [34] is negligible, if observed at all. In contrast, vigorous gas evolution was always observed when MCMB electrodes were polarized in any Li salt ($LiClO_4$, $LiPF_6$)/alkyl carbonate (EC–DMC, PC, EC–PC) solutions.

Fig. 6 shows typical AFM images obtained *in situ* from MCMB electrodes at OCP (≈3 V) and after polarization to 0.3 V (Li/Li$^+$) in 1 M LiBOB and 1M $LiPF_6$ solutions, as indicated. There are pronounced morphological changes due to the cathodic polarization of both electrodes connected with the formation of surface films. A clear result from these measurements, reflected also in the images of Fig. 6, are the much rougher surface films formed in $LiPF_6$ solutions. Table 1 compares the calculations of surface roughness of MCMB electrodes polarized to 1 and 0.3 V in $LiPF_6$ and LiBOB solutions, calculated from the AFM images. The roughness average $R_a$ in the table, is the arithmetic average of the absolute values of the surface height:

$$R_a = \frac{1}{N}\sum_{i=1}^{N} Z_i,$$

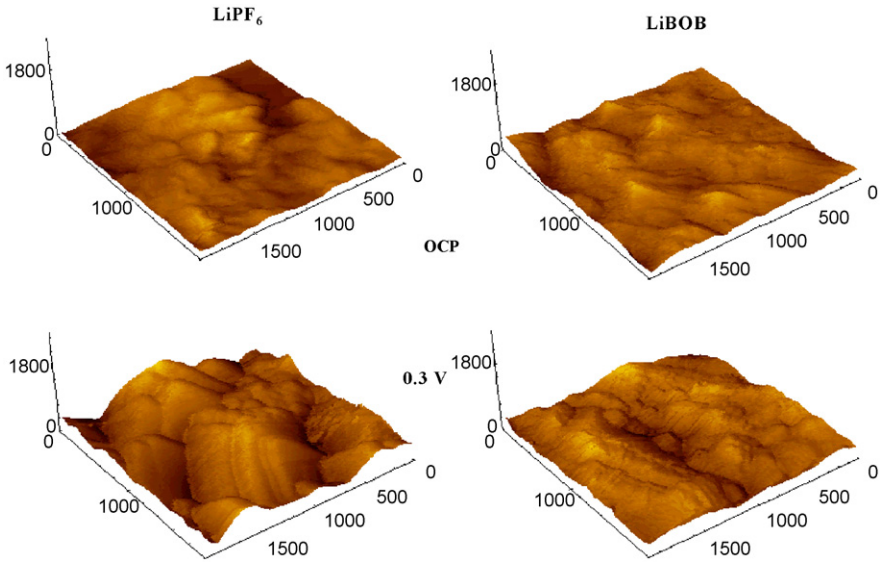


Fig. 6. AFM images (2 μm × 2 μm) of MCMB electrodes obtained *in situ* in 1 M LiBOB and 1 M $LiPF_6$ solutions in EC–PC 2:3 at OCP and after polarization to 0.3 V (vs. $Li/Li^+$). The potentials are indicated.

Table 1
Roughness average of MCMB electrodes at OCP after being polarized in EC–PC 2:3 solutions to 1 and 0.3 V, calculated from the AFM images

| Experiment 1 (AFM images 4 μm × 4 μm) | | | | |
|---|---|---|---|---|
| Salt | OCP | | 1 V | |
| | $R_a$ (nm) | σ (nm) | $R_a$ (nm) | σ (nm) |
| LiPF6 | 424.3 | 106.5 | 443.8 | 132.5 |
| LiBOB | 438.2 | 99.3 | 276.5 | 62.9 |
| **Experiment 2 (AFM images 2 μm × 2 μm)** | | | | |
| Salt | OCP | | 0.3V | |
| | $R_a$ (nm) | σ (nm) | $R_a$ (nm) | σ (nm) |
| LiPF6 | 84.6 | 27.3 | 287.3 | 86.9 |
| LiBOB | 123.8 | 34.8 | 193.0 | 58.3 |

where $Z_i$ is the height at a point $i$, $N = 65{,}536$ ($256^2$) is the number of data points;
and σ is the standard deviation of the height :

$$\sigma = \sqrt{\frac{1}{N-1}\sum_{i=1}^{N}(Z_i - R_a)^2}.$$

Table 1 belongs to two sets of measurements, denoted as experiment 1 and experiment 2, in which the images for calculation were 4 μm × 4 μm and 2 μm × 2 μm, respectively. Hence, the starting point (roughness at OCP) was different in each experiment. The results in this table, which are typical to all the experiments performed, clearly demonstrate that the surface films formed on MCMB electrodes in LiBOB solutions are much less rough compared to those formed in $LiPF_6$ solutions. We explain this finding by the fact that LiBOB is reduced at a relatively high potential and its reduction products (see suggestions in Scheme 1) precipitate (at least in part) on the electrodes' surface, thus attenuating any other possible reduction processes that occur at lower potentials, e.g., solvent reduction. The possible secondary reactions of surface species initially formed in $LiPF_6$ solutions with HF may also contribute to a relatively high roughness of the surface films formed on electrodes in these solutions.

The last subject dealt with herein is a comparison between the thermal stability of LiBOB and $LiPF_6$ solutions in contact with Li metal as a probe.

Fig. 7a compares heat flow from systems comprised lithium (0.6 mg Li versus 3 μl solution) and 1 M $LiPF_6$ solutions (in PC and in EC–DMC 1:1), during the course of being heated up to 350 °C. Fig. 7b shows similar results from similar experiments with 1 M LiBOB solutions, as indicated. The experiments with the $LiPF_6$ solutions show that when the solvent is a EC–DMC mixture, a thermal reaction starts above 150 °C (due to the red-ox behavior of all $LiPF_6$ solutions in organic solvents at elevate temperatures) and accelerates upon the melting of the lithium at >180 °C. Our results correlates with the ARC studies that shows lower reactivity of LiBOB/EC:DEC electrolytes with lithiated graphite [14] and with $Li_{0.81}C_6$ electrodes [35] than $LiPF_6$-based electrolytes. When the solution is PC, a very pronounced thermal reaction is developed immediately as Li melts. When comparing the heat flow versus $T$ curves in Fig. 7a and b, it is clear that LiBOB solutions and their lithium passivity are much more thermally stable than $LiPF_6$ solutions. For instance, the thermal reaction of an EC–DMC/LiBOB solution with lithium does not start as soon as the lithium melts, but rather at a temperature 5–10 °C higher than that of the Li melting point. This means that the passivation of active (reducing) surfaces in LiBOB solutions is so efficient that it can, to some extent, protect even liquid lithium. These studies also demonstrate the pronounced influence of the solvent used on the systems' thermal stability. However, this subject is beyond the scope of this paper.

All of the results presented above demonstrate the unique behavior of LiBOB solutions compared to all the other Li salt solutions that are commonly used in Li-ion batteries.

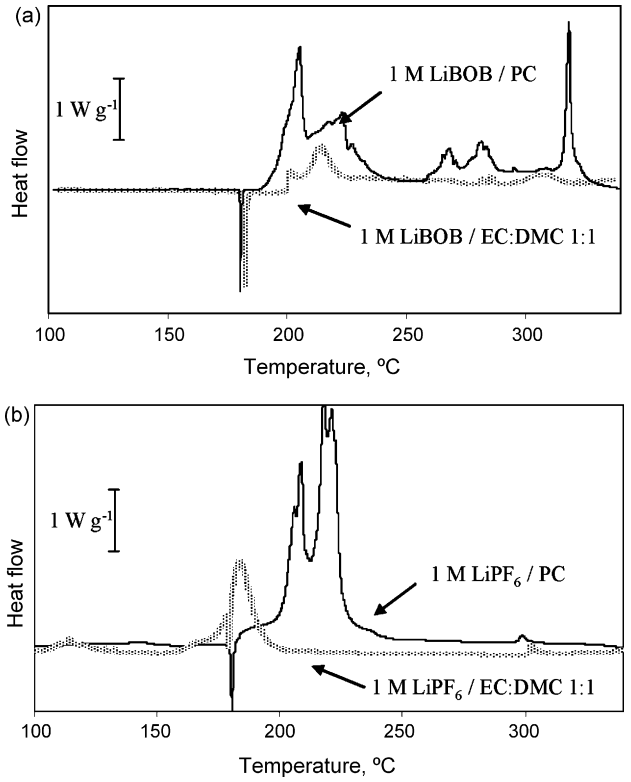


Fig. 7. DSC curves (heat flow vs. *T*) obtained upon heating samples containing lithium metal and alkyl carbonate-based solutions: (a) 1 M LiBOB solutions in PC and in EC–DMC 1:1, as indicated, (b) 1 M $LiPF_6$ solutions in PC and EC–DMC. The heating rate is 1 °C $min^{-1}$.

## 4. Conclusions

The studies of non-active Ni electrodes, composite graphite electrodes and metallic lithium in LiBOB solutions (alkyl carbonate mixtures), compared to the commonly used $LiPF_6$ solutions, and the use of several techniques such as EQCM, FTIR, XPS, *in situ* AFM, and DSC, in conjunction with electrochemical measurements, clearly demonstrated the following unique behavior of LiBOB solutions:

1. LiBOB participates in the surface chemistry of lithium, lithiated graphite and non-active metal electrodes polarized to low potentials, even when the solvents are highly electrophilic and reactive, as in the case of cyclic alkyl carbonates.
2. The onset potential of the LiBOB surface reactions is higher than that of alkyl carbonates, and therefore, when graphite electrodes are polarized cathodically, LiBOB is reduced first (>1.7 V versus $Li/Li^+$), and the surface species thus formed attenuate all the other possible surface reactions of solution species.It should be noted that the above two conclusions are well in line with all previous studies of LiBOB solutions by others.
3. *In situ* studies by AFM showed that the morphology of the surface films formed on graphite electrodes in LiBOB solutions is smoother than that of surface films formed in $LiPF_6$ solutions. The accompanying gas evolution is negligible in the cases of LiBOB solutions. This conclusion is valid for both PC and EC–DMC solutions.
4. Thermal studies also demonstrated a superior thermal stability of LiBOB solutions and surface films formed on lithium in these solutions, compared to all the thermal stability aspects of the commonly used $LiPF_6$ solutions.

## References

[1] S.E. Sloop, J.B. Kerr, K. Kinoshita, J. Power Sources 119 (2003) 330.
[2] J.S. Gnanaraj, E. Zinigrad, L. Asraf, H.E. Gottlieb, M. Sprecher, M. Schmidt, W. Geissler, D. Aurbach, J. Electrochem. Soc 150 A (2003) 1533.
[3] J. Jiang, J.R. Dahn, Electrochem. Solid-State Lett. 6 (2003) A180.
[4] J. Jiang, J.R. Dahn, Electrochem. Electrochim. Acta 49 (2004) 2661.
[5] E. Zinigrad, L. Larush-Asraf, J.S. Gnanaraj, M. Sprecher, D. Aurbach, Thermochimica Acta 438 (2005) 184.
[6] M. Schmidt, U. Heider, A. Kuehner, R. Oesten, M. Jungnitz, N. Ignat'ev, P. Sartori, J. Power Sources 97–98 (2001) 557.
[7] S. Leroy, F. Blanchard, R. Dedryvere, H. Martinez, B. Carre, D. Lemordant, D. Gonbeau, Surf. Interface Anal. 37 (2005) 773.
[8] J. Chen, L.F. Wang, B.J. Fang, S.Y. Lee, R.Z. Guo, J. Power Sources 157 (2006) 515.
[9] G.G. Amatucci, J.M. Tarascon, L.C. Klein, Solid State Ionics 83 (1996) 167.
[10] S.E. Sloop, J.K. Pugh, S. Wang, J.B. Kerr, K. Kinoshita, Electrochem. Solid-State Lett. 4 (2001) A42.
[11] J.S. Gnanaraj, M.D. Levi, Y. Gofer, D. Aurbach, J. Electrochem. Soc. 150 (2003) A445.
[12] J.S. Gnanaraj, E. Zinigrad, L. Asraf, H. Gottlieb, M. Sprecher, M. Schmidt, W. Geissler, D. Aurbach, Electrochem. Commun. 5 (2003) 946.
[13] S.S. Zhang, K. Xu, T.R. Jow, J. Power Sources 154 (2006) 276.
[14] J. Jiang, J.R. Dahn, Electrochem. Electrochem. Solid-State Lett. 6 (A180) (2003).
[15] G.V. Zhuang, K. Xu, T.R. Jow, P.N. Rosss, Electrochem. Solid-State Lett. 7 (2004) A224.
[16] K. Xu, S.S. Zhang, T.R. Jow, Electrochem. Solid-State Lett. 6 (2003) A117.
[17] K. Xu, U. Lee, S.S. Zang, J.L. Allen, T.R. Jow, Electrochem. Solid-State Lett. 7 (2004) A273.
[18] K. Xu, U. Lee, S.S. Zang, T.R. Jow, J. Electrochem. Soc. 151 (2004) A2106.
[19] K. Xu, S. Zhang, R. Jow, J. Power Sources 143 (2005) 197.
[20] Z. Chen, W.Q. Lu, J. Lu, K. Amine, Electrochim. Acta 51 (2006) 3322.
[21] D. Aurbach, M.D. Levi, E. Levi, A. Schechter, J. Phys. Chem. B 101 (1997) 2195.
[22] D. Aurbach, Y. Cohen, J. Electrochem. Soc. 143 (1996) 3525.
[23] D. Aurbach, Yaron Cohen, J. Phys. Chem. B 104 (2000) 12282.
[24] D. Aurbach, B. Markovsky, A. Rodkin, M. Cojocaru, E. Levi, H.J. Kim, Electrochim. Acta 47 (2002) 1899.
[25] D. Aurbach, M.L. Daroux, P. Faguy, E. Yeager, J. Electroanal. Chem. 297 (1991) 225.
[26] D. Aurbach, J. Electrochem. Soc. 136 (1989) 906.
[27] L.-F. Li, D. Totir, Y. Gofer, G.S. Chottiner, D.A. Scherson, Electrochem. Acta 44 (1998) 949.
[28] D. Aurbach, Y. Gofer, M. Ben-Zion, P. Aped, J. Electroanal. Chem. 339 (1992) 451.
[29] M. Moshkovich, Y. Gofer, D. Aurbach, J. Electrochem. Soc. 148 (2001) E155.
[30] D. Aurbach, B. Markovsky, A. Schechter, Y. Ein-Eli, H. Cohen, J. Electrochem. Soc. 143 (1996) 3809.
[31] NIST Chemistry WebBook http://webbook.nist.gov.
[32] D. Aurbach, M.L. Daroux, P. Faguy, E. Yeager, J. Electrochem. Soc. 134 (1987) 1611.
[33] J.-C. Panitz, U. Wietelmann, M. Wachtler, S. Strobele, M. Wohlfahrt-Mehrens, J. Power Sources 153 (2006) 396.
[34] R. Imhof, P. Novak, J. Electrochem. Soc. 145 (1998) 1081.
[35] J. Jiang, H. Fortier, J.N. Reimers, J.R. Dahn, J. Electrochem. Soc. 151 (2004) A609.